JOURNAL OF THE ROYAL SOCIETY Interface

J. R. Soc. Interface (2006) **3**, 495–505
doi:10.1098/rsif.2005.0108
Published online 27 December 2005

Electrochemical properties of 316L stainless steel with culturing L929 fibroblasts

Sachiko Hiromoto* and Takao Hanawa†

Reconstitution Materials Group, Biomaterials Center, National Institute for Materials Science, 1-1 Namiki, Tsukuba 305-0044, Japan

Potentiodynamic polarization and impedance tests were carried out on 316L stainless steel with culturing murine fibroblast L929 cells to elucidate the corrosion behaviour of 316L steel with L929 cells and to understand the electrochemical interface between 316L steel and cells, respectively. Potential step test was carried out on 316L steel with type I collagen coating and culturing L929 cells to compare the effects of collagen and L929 cells. The open-circuit potential of 316L steel slightly shifted in a negative manner and passive current density increased with cells, indicating a decrease in the protective ability of passive oxide film. The pitting potential decreased with cells, indicating a decrease in the pitting corrosion resistance. In addition, a decrease in diffusivity at the interface was indicated from the decrease in the cathodic current density and the increase in the diffusion resistance parameter in the impedance test. The anodic peak current in the potential step test decreased with cells and collagen. Consequently, the corrosion resistance of 316L steel decreases with L929 cells. In addition, collagen coating would provide an environment for anodic reaction similar to that with culturing cells.

Keywords: stainless steel; fibroblast cells; collagen; biomaterials; electrochemical measurement

1. INTRODUCTION

In the early stage of implantation of biomaterials in the human body, immunocytes, such as macrophages and lymphocytes, accumulate around the materials, and the adhesion of cells, such as fibroblasts and osteoblasts, follows thereafter (Matsumoto 1978). Cells adhere on the surface through the points of contact with cell-adhesive proteins (Hayashi 1995), which make a gap of a nanometre order between the cells and the material. Cells generate various chemicals, such as cytokines (growth factor) and inorganic ions (Alberts *et al.* 2002). In addition, the cells generate various kinds of extracellular matrixes (ECM; Hayashi 1995; Lanza *et al.* 1997). In the ECM, polysaccharides form a gel-like basement containing a lot of water as well as fibrous proteins and cell-adhesive proteins (Alberts *et al.* 1990). Water in the gel-like basement governs the diffusion of molecules (Alberts *et al.* 1990). Those cell adhesion mechanisms and cell products appear to influence the chemical properties of a solution over the material. Gilbert *et al.* (1998) suggested the diffusion retardation of dissolved oxygen near osteoblast cells on Ti because, after the consumption of dissolved oxygen on the surface by cathodic polarization, the recovery of dissolved oxygen concentration delayed near cells. Hiromoto & Hanawa (2004) found a decrease in pH from 7.5 to 5.2 to 6.8 near fibroblast L929 cells on 316L steel and Ti using a tungsten micro probe. The results indicate that the corrosion behaviour of metallic biomaterials should be affected with cells, such as osteoblasts and fibroblasts, and their ECM.

In order to examine the effect of cells on the corrosion behaviour of metallic biomaterials, osteoblasts or fibroblasts are often used. Both osteoblasts and fibroblasts generate collagen as a main component of ECM (Kuboki *et al.* 1992; Lanza *et al.* 1997). The osteoblast MC3T3-E1 cell generates a high concentration of collagen type I, and mineralization initiates after a certain amount of collagen is accumulated (Kuboki *et al.* 1992). When mineralization on collagen fibres does not initiate with osteoblasts, the concentration of precipitated calcium phosphate on Ti with osteoblast-like cells derived from the human mandibular bone is 1–2 at.%, which is in the same magnitude as that on Ti with murine fibroblast L929 incubated on it (Mustafa *et al.* 2002; Hiromoto *et al.* 2004). This indicates that osteoblasts and fibroblasts probably form similar interface structures under a cell culture environment and the results obtained using these cells are comparable when osteoblasts do not initiate mineralization.

The effects of cells on the surface composition of metallic biomaterials are investigated using several kinds of cells (Sundgren *et al.* 1986; Esposito *et al.* 1999; Hanawa *et al.* 2001, 2002; Takemoto *et al.* 2002;

*Author for correspondence (hiromoto.sachiko@nims.go.jp).
†Present address: Institute of Biomaterials and Bioengineering, Tokyo Medical and Dental University, 2-3-10 Kanda-Suruga-dai, Chiyoda-ku, Tokyo 101-0062, Japan.

Received 13 September 2005
Accepted 29 November 2005

Table 1. Chemical composition of 316L stainless steel (mass%).

C	Si	Mn	P	S	Ni	Cr	Mo	Fe
0.019	0.48	1.18	0.038	0.013	12.10	16.72	2.05	balance

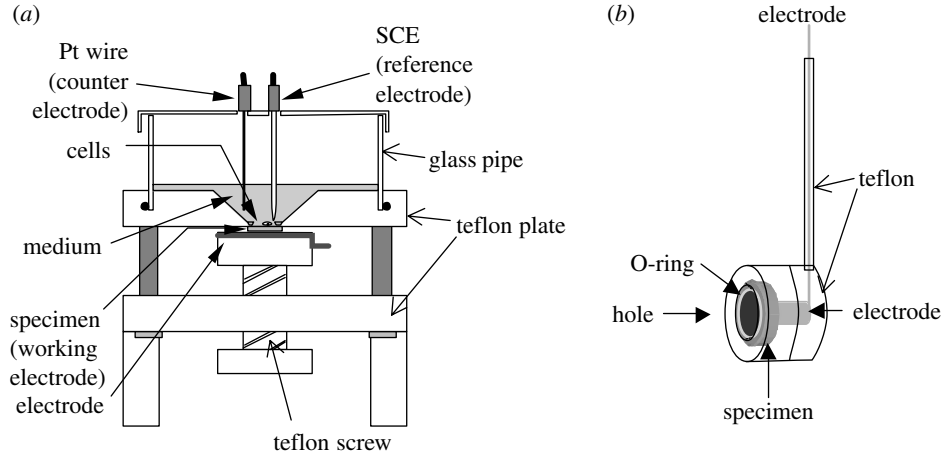

Figure 1. Schematics of (*a*) electrochemical cell for cell culture and (*b*) electrode holder.

Vinnichenko *et al.* 2002; Aoyagi *et al.* 2004). Vinnichenko *et al.* (2002) found that, on the surface of stainless steel, Ni migrates into the adsorbed protein layer and the Cr content increased after culturing fibroblast L929 and osteosarcoma SAOS-2. They estimated that the thickness of the adsorbed protein layer on stainless steel as 2.5–6.0 nm after the cells had been removed by trypsin (Vinnichenko *et al.* 2002). Aoyagi *et al.* (2004) analysed the composition of the protein layers on 316L steel and Ti formed with and without L929 cells with time of flight–secondary ion mass spectroscopy (TOF–SIMS) and confirmed the difference in composition of the protein layer with and without cells. Hanawa *et al.* (2001) and Hiromoto *et al.* (2002*a*,*b*, 2004) found that the precipitation of calcium phosphate on 316L steel, Co–Cr–Mo alloy, and Ti decreases with L929 cells. They also found that sulphur is incorporated in the surface oxide film as sulphite and/or sulphide only when L929 cells are cultured on 316L steel and Ti (Hanawa *et al.* 2002; Hiromoto *et al.* 2004). The incorporation of sulphur is also observed on stainless steel and Ti–6Al–4V alloy retrieved from soft tissues (Sundgren *et al.* 1986) and on Ti–6Al–4V alloy from hard tissues, such as human jaw and bone marrow (Sundgren *et al.* 1986; Esposito *et al.* 1999; Takemoto *et al.* 2002). Esposito *et al.* (1999) suggested that the sulphur originates from proteoglycans generated by cells, although the chemical state of sulphur is not analysed.

The electrochemical measurement of metallic biomaterials with culturing cells is increasing (Messer *et al.* 2001; Hiromoto *et al.* 2002*a*,*b*). Hiromoto *et al.* (2002*a*,*b*) found that the cathodic current density on Ti decreases with L929 cells in polarization test, and, according to the fitting calculation of parameters in an equivalent circuit based on alternating current (AC) impedance test, the diffusion resistance at the interface increases with L929 cells. In addition, they performed the same experiment at different temperatures and found that the impedance behaviour at the interface on Ti changes with temperature (Hiromoto *et al.* 2002*a*,*b*). Messer *et al.* (2001) found that the corrosion rate of the metallic material increases with human gingival fibroblasts. Mustafa *et al.* (2002) performed electrochemical impedance measurement of Ti with culturing osteoblast-like cells and found that the osteoblast-like cell does not significantly influence the corrosion resistance of Ti.

The results above indicate that the cells affect the corrosion behaviour of metallic biomaterials. However, the corrosion mechanism of metallic biomaterials with cells is not yet understood. The understanding of the corrosion mechanism with cells must contribute to improve corrosion resistance of metallic biomaterials, which ultimately leads to a decrease in the toxicity problem and fretting corrosion wear. In addition, the obtained results are useful for the establishment of proper evaluation conditions for metallic biomaterials *in vitro*. In this study, several electrochemical measurements were performed on 316L steel with and without culturing L929 cells to understand the corrosion behaviour of 316L steel with cells on it. L929 cells were employed because 316L steel is used in bone plates and stents that attach to hard and soft tissues in the body, respectively.

2. MATERIAL AND METHODS

2.1. Preparation of specimen

Austenitic 316L stainless steel (316L steel) was employed. The composition is summarized in table 1. Disks of 316L steel with a diameter of 20 mm and a thickness of 1 mm were finished with a #600 grid SiC paper (Buehler Co.) and ultrasonically rinsed with distilled water and acetone.

2.2. Polarization and impedance test

The 316L steel disk specimen was mounted on an electrochemical cell for cell culture (see figure 1*a*;

Table 2. Compositions of Hanks and MEM+FBS (mol l^{-1}).

composition	Hanks	MEM+FBS
NaCl	1.37×10^{-1}	1.04×10^{-1}
KCl	5.37×10^{-3}	4.82×10^{-3}
$CaCl_2$	1.26×10^{-3}	1.62×10^{-3}
Na_2HPO_4	4.23×10^{-4}	8.08×10^{-4}
KH_2PO_4	4.41×10^{-4}	—
Mg_2SO_4	7.39×10^{-4}	7.30×10^{-4}
$NaHCO_3$	4.17×10^{-3}	2.14–2.36×10^{-2}
amino acid		5.0×10^{-3}
protein/g l^{-1}		<10

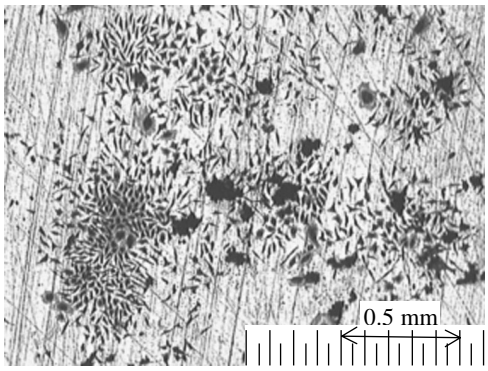

Figure 2. Optical image of the surface of 316L steel with culturing murine fibroblasts L929 for 7 days.

Hiromoto *et al.* 2002*a*,*b*). The entire electrochemical cell mounting specimen was sterilized by autoclaving with saturated water vapour at 393 K for 30 min.

Murine fibroblast L929 cells were seeded on a disk with 10 µl of suspension of 5000 cells and Eagle's minimum essential medium with 10 vol% of foetal bovine serum (MEM+FBS). Subsequently, 8 ml of MEM+FBS was poured gently along the slope of the hole. The L929 cells were cultured in an incubator with an atmosphere of air containing 5% CO_2 at 310 K for 7 days. In order to observe the coverage of the 316L steel disk with cells, the cells were fixed on the disk by dehydration with methanol and stained violet with a Giemsa reagent. Subsequently, the disk surface was observed with an optical microscope.

As a reference, 8 ml of MEM+FBS or Hanks' solution (Hanks) was poured on a 316L steel disk mounted on the electrochemical cell and kept for 7 days in an incubator. MEM+FBS contains inorganic ions and organic biomolecules of proteins and amino acids. Hanks contains only inorganic ions. Table 2 shows the compositions of MEM+FBS and Hanks. The disks with culturing cells are described as L929/316L, and those immersed in MEM+FBS and Hanks are described as MEM+FBS/316L and Hanks/316L, respectively.

After 7 days incubation, the electrochemical cell was moved in an adiabatic styrene-foam box from an incubator, and a platinum wire counter electrode and a saturated calomel reference electrode (SCE) were subsequently mounted. The temperature of the electrochemical cell was kept by circulating water at 310 K

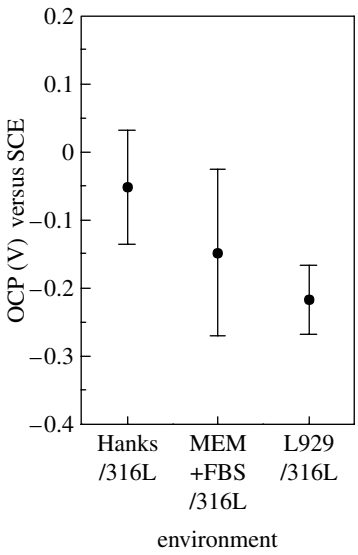

Figure 3. Open-circuit potentials (OCP) of 316L steel in various environments.

around the electrochemical cell. The potential of the specimen was monitored over 30 min, and the stabilized potential was used as the open-circuit potential (OCP).

In the polarization test, the potential of 316L steel was both anodically and cathodically swept from the OCP at a rate of 20 mV min^{-1} using a potentiostat (ALS660 electrochemical analyser). In the AC impedance test, the 316L steel was kept at the OCP, and a sinusoidal potential with a 5 mV amplitude for the frequency region of 10^5–10^{-3} Hz was applied using a frequency response analyser (ALS660 electrochemical analyser). The same measurements were performed at least three times in each environment.

2.2. Potential step test

The 316L steel disks finished with #600 SiC paper were treated by autoclaving with saturated water vapour at 393 K for 30 min. The specimen after autoclaving treatment is described as Autoclaved 316L. A part of the Autoclaved 316L was incubated with L929 cells in 5 ml of MEM+FBS for 7 days in a six-well cell culture dish. Another part of the Autoclaved 316L was immersed in 5 ml of Hanks or MEM+FBS for 7 days in a six-well cell culture dish. The other part of the Autoclaved 316L was coated with collagen (type I, KOKEN Co., Ltd) according to the following procedure. A 0.03%-collagen/HCl solution of pH 3.0 was prepared in cold water. The autoclaved 316L steel disk was immersed in the collagen solution overnight. Subsequently, the disk was removed from the solution and rinsed with a phosphate-buffered saline solution. The disk with L929 cells incubated on it is described as L929/316L, and the disks immersed in MEM+FBS and Hanks are described as MEM+FBS/316L and Hanks/316L, respectively. The disk with collagen coating is described as Collagen/316L.

The disk was removed from the cell culture dish and mounted in the electrode holder with an O-ring (see figure 1*b*). Subsequently, the disk was immersed in 500 ml of MEM+FBS gently bubbled with N_2 gas for

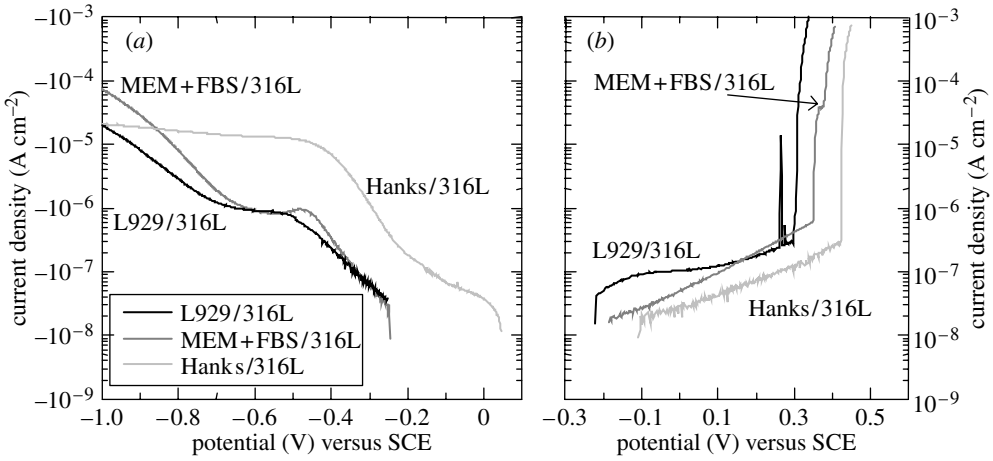

Figure 4. (*a*) Cathodic and (*b*) anodic polarization curves of 316L steel in various environments.

60 min and kept at 310 K. MEM+FBS was used as an electrolyte to avoid the desorption of biomolecules from MEM+FBS/316L and L929/316L during polarization. The OCP of the 316L steel was about −0.2 V (SCE). The potential of 316L steel was then stepped to −1.0, −0.5, 0, 0.05 or 0.1 V from OCP, respectively, and kept until the induced current showed a constant value. The potential values of −1.0 and −0.5 V are in the cathodic regions, and those of 0, 0.05 and 0.1 V are in the passive regions on measured polarization curves. A potentiogalvanostat (Hokuto-Denko, HZ3000) was used in this test. The current acquisition period was 50 ms.

3. RESULTS

3.1. Optical image

Figure 2 shows the optical image of the surfaces of 316L steel with fixed and stained L929 cells. The surface of 316L steel is not uniformly covered with L929 cells, and the cells form colonies. The cells are not arranged along the scratches and expand independently of the scratches. No corrosion product is observed, except for scratches resulting from polishing.

3.2. OCP

Figure 3 shows the OCP values of 316L steel in various environments. The average of OCP in Hanks is −0.05 V (SCE) and decreases by *ca* 0.1 V with biomolecules and L929 cells.

3.3. Potentiodynamic polarization test

Figure 4 shows the cathodic and anodic polarization curves of 316L steel in various environments. When the current density is less than 10^{-7} A cm^{-2}, a noise current is observed because of the resolution limit of the potentiostat. The cathodic current density of Hanks/316L increases from OCP to −0.4 V, while the rate of the current increase changes at −0.2 V. In a potential region lower than −0.4 V, the current density is nearly constant up to −1.0 V. The cathodic current densities of MEM+FBS/316L and L929/316L increase from OCP to −0.4 V and are constant up to −0.65 V, following an increase from −0.65 V. The cathodic current density around OCP decreases with biomolecules and L929 cells.

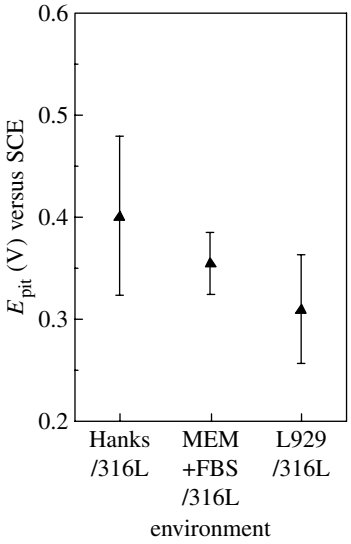

Figure 5. Pitting potentials (E_{pit}) of 316L steel in various environments.

In the anodic polarization test, all specimens are spontaneously passivated with the increase in potential, and the currents show an abrupt increase in the potential region from 0.3 to 0.5 V. The passive current density increases with biomolecules and L929 cells.

Since several pits were observed on the surface after the anodic polarization, the abrupt increase on the anodic current originated from the pitting corrosion. The potential at which the current density abruptly increases was obtained as a pitting potential (E_{pit}) and is summarized in figure 5. The average of E_{pit} decreases by *ca* 40 mV with biomolecules and L929 cells.

3.4. Potential step test

When the potential of a specimen is stepped from OCP to a certain potential (E_{ch}), the anodic or cathodic current abruptly increases to reach a peak value (J_{peak}) and subsequently comes to a constant value ($J_{const.}$). Figure 6 shows typical anodic and cathodic current

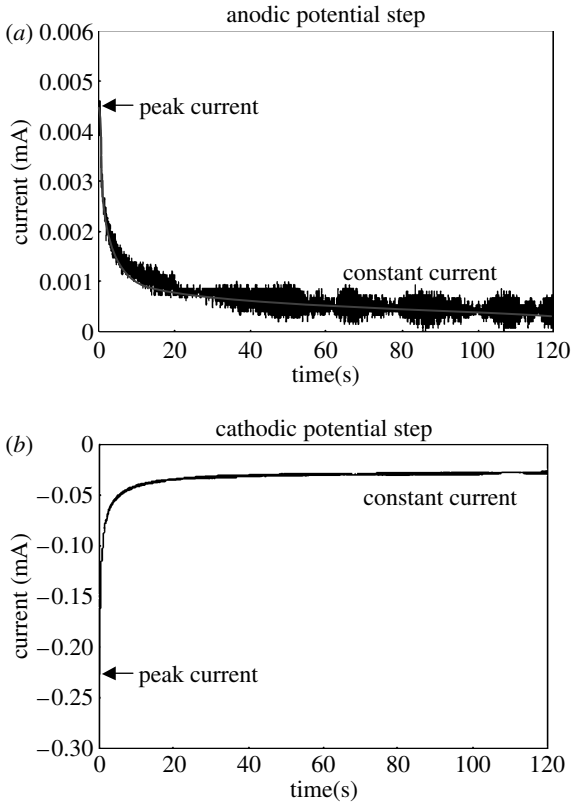

Figure 6. Typical (*a*) anodic and (*b*) cathodic current transient curves in potential step test.

transient curves. The J_{peak} values under various conditions are summarized in figure 7*a*. The J_{peak} value is generally influenced by the charge transfer behaviour and capacitance at the interface (Tamamushi 2000). The $J_{const.}$ values are summarized in figure 7*b*. However, the $J_{const.}$ values of Hanks/316L, Autoclaved 316L, and Collagen/316L are not discussed in this study because the biomolecules in MEM+FBS adsorb on the surface during polarization although the original surfaces do not have the adsorbed biomolecules in MEM+FBS. The adsorption amount and conformation of proteins, such as albumin and fibrinogen, change with the potential (Stoner & Srinivasan 1970; Ivarsson & Lundstrom 1986). In addition, adsorbed small proteins are replaced with large proteins with time (Vroman effect; Wahlgren *et al.* 1991). The change in the adsorbed biomolecules during polarization prevents the understanding of the constant current density.

When the J_{peak} values of Hanks/316L, MEM+FBS/316L, and L929/316L are compared, the J_{peak} value at −0.5 V is observed to decrease with L929 cells, while there is not a significant difference in the J_{peak} values at −1.0 V. Under the anodic charge, the J_{peak} value increases with biomolecules and L929 cells.

When the J_{peak} values of Autoclaved 316L and Collagen/316L are compared, the J_{peak} value at −0.5 V does not show a significant difference with collagen, while the J_{peak} value at −1.0 V decreases with collagen. Under the anodic charge, the J_{peak} value increases with collagen.

The $J_{const.}$ value at −0.5 V slightly decreases with L929 cells, while that at −1.0 V slightly increases with cells. The $J_{const.}$ values under an anodic charge of L929/316L are larger than those of MEM+FBS/316L.

3.5. Impedance test

Figure 8 shows the impedance spectra (Bode plots) of L929/316L, MEM+FBS/316L, and Hanks/316L. On Hanks/316L, the impedance (Z) curve (see figure 8*a*) shows a very small plateau region, and the phase shift (θ) curve (see figure 8*b*) shows a slight decrease at 5×10^{-2} Hz, indicating that there are two time constants on Hanks/316L. On the other hand, the impedance spectra of L929/316L and MEM+FBS/316L do not show apparent two time constants.

The interface structures of 316L steel in various environments are assumed as shown in figure 9*a*–c based on surface analysis data of 316L steel prepared in the same procedure as that in this study (Hanawa *et al.* 2002). The interface structures and an equivalent circuit on Ti with and without culturing L929 cells were assumed elsewhere (Hiromoto *et al.* 2002*a*,*b*). The interface structures and impedance spectra on 316L steel are similar to those on Ti. The same interface model and equivalent circuit were then applied for the results on 316L steel. The assumed equivalent circuit is shown in figure 9*d*. The employed equivalent circuit has a Warburg coefficient (W_b) that represents a diffusion resistance. The curve fitting was carried out on all the specimens using the least squares approximation. The measured curves and fitted curves on L929/316L and MEM+FBS/316L show a good coincidence except for the high-frequency region, as shown in figure 10. The error in the high-frequency region is due to the delay of the frequency response of the analyser. However, on Hanks/316L, the fitted curves do not coincide with the measured curves.

The approximated resistance (R_b), capacitance (C_b), and Warburg coefficient (W_b) of the biomolecule adsorption layer and the capacitance of the surface oxide film (C_f) are summarized in figure 11. The approximated R_b value ranges from 10^3 to $10^5\,\Omega\,cm^2$, and the R_b increases with L929 cells. The approximated resistance of the surface oxide film (R_f) ranges from 10^6 to $10^8\,\Omega\,cm^2$. The effect of L929 cells on R_f value is not discussed because the R_f value is the extrapolated value. The existence of L929 cells does not cause a significant change in the approximated C_b and C_f values. The approximated C_b value ranges from 0.3×10^{-4} to $5\times10^{-4}\,F\,cm^{-2}$. These C_b values are equivalent to the capacitance of adsorbed albumin, fibrinogen, and thrombin on Pt, 0.1×10^{-4} to $1\times10^{-4}\,F\,cm^{-2}$ (Stoner & Srinivasan 1970; Lacour *et al.* 1991). The approximated C_f value ranges from 2×10^{-5} to $8\times10^{-5}\,F\,cm^{-2}$. These C_f values are equivalent to the capacitance of 316L steel in fresh river water, 2×10^{-5} to $5\times10^{-5}\,F\,cm^{-2}$ (Dickinson *et al.* 1996). These results indicate that the approximation of measured data to the equivalent circuit (see figure 9*d*) is acceptable. The approximated W_b value ranges from 4×10^4 to $8\times10^6\,\Omega\,cm^2$. These W_b values are almost equivalent to those of Ti, 3×10^4 to $2\times10^6\,\Omega\,cm^2$ (Hiromoto *et al.* 2002*b*). The W_b value

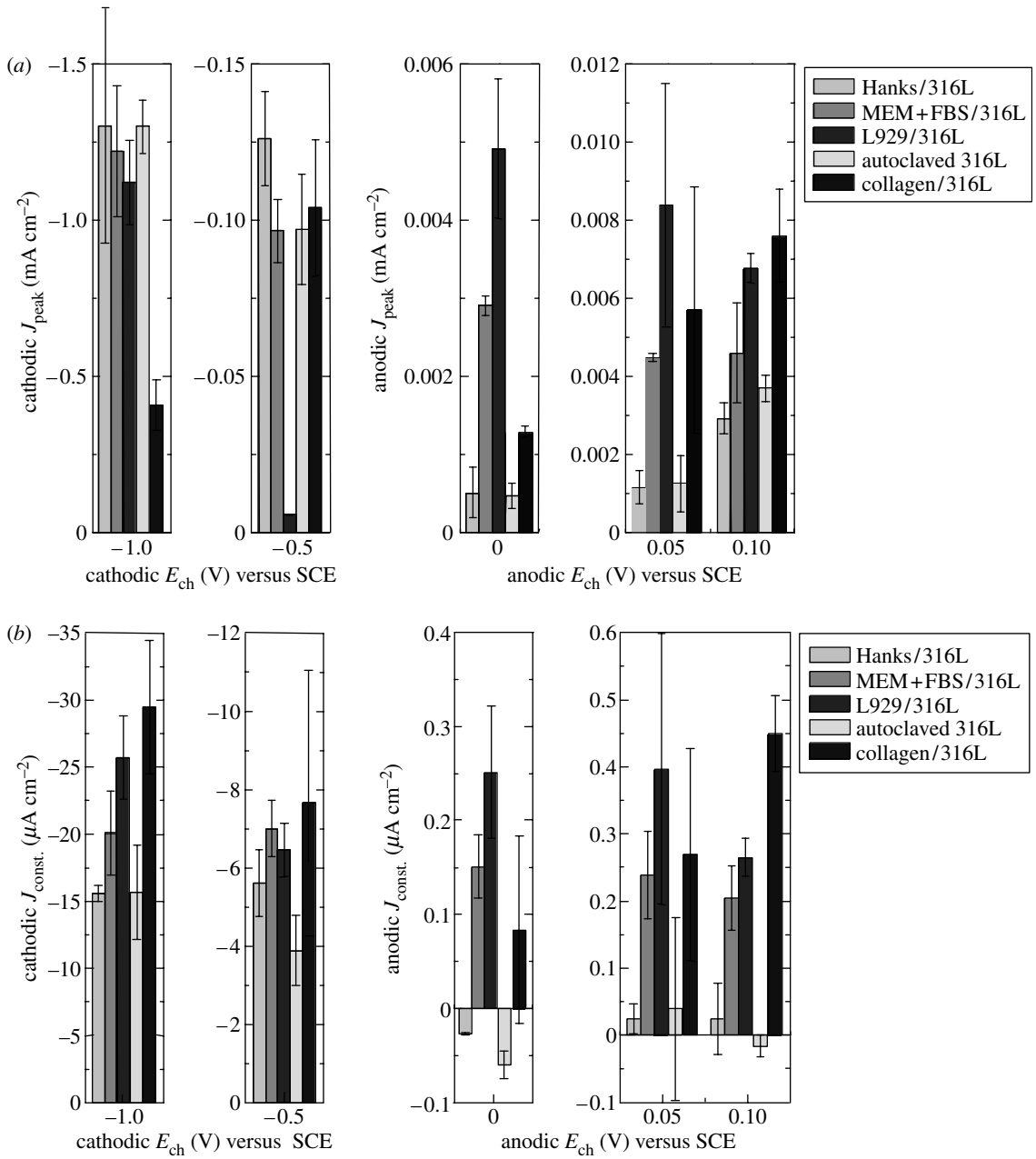

Figure 7. Cathodic and anodic (*a*) peak current density (J_{peak}) and (*b*) constant current density ($J_{const.}$) obtained from current transient curves on specimens prepared under various conditions.

increases with L929 cells, indicating that the diffusivity at the interface decreases with L929 cells.

4. DISCUSSION

4.1. Effects of biomolecules and L929 cells on the cathodic reaction

In the potential region from OCP to −0.6 V, where the reduction of dissolved oxygen occurs (Pourbaix 1974), the cathodic current densities (see figures 4 and 6) decrease with biomolecules and cells. In addition, the cathodic polarization curves of L929/316L and MEM+FBS/316L in this potential region show a constant value, which is probably a diffusion-limiting current. The approximated W_b value increases with cells (see figure 11). These results indicate that the adsorbed biomolecules and adhering cells prevent the diffusion of dissolved oxygen at the interface on 316L steel. The prevention of diffusion with L929 cells is also suggested on Ti (Hiromoto *et al.* 2004). In addition, Gilbert *et al.* (1998) reported the prevention of dissolved oxygen diffusion near osteoblast-like cells on Ti.

Interestingly, the J_{peak} at −0.5 V significantly decreases, and the $J_{const.}$ at −0.5 V slightly decreases with cells (see figure 7). On the other hand, the J_{peak} at −0.5 V of Collagen/316L is lower than that of autoclaved specimen, indicating that collagen does not cause a decrease in the J_{peak} at −0.5 V. It is possible that the oxygen concentration near cells decreases with the consumption by cells, leading to a decrease in the cathodic current density at −0.5 V with cells.

In the lower-potential region, where a reduction of H^+ occurs (Pourbaix 1974), there is not a significant difference in the J_{peak} values at −1.0 V with and

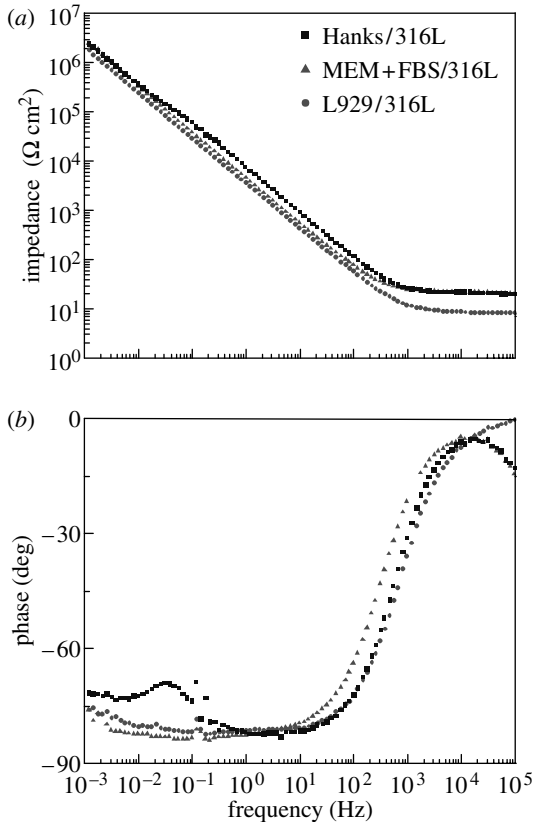

Figure 8. (*a*) Impedance (Z) and (*b*) phase shift (θ) dependence on frequency (Bode plot) of 316L steel in various environments.

without biomolecules and L929 cells (see figure 7*a*). However, especially with coated collagen, the J_{peak} value at −1.0 V significantly decreases. This result indicates that the coverage of the surface with collagen diminishes the H^+ reduction reaction. According to the structure of collagen type I, hydrophobic amino acid residues are exposed on the surface (Lanza *et al.* 1997). The exposed amino acid residues might influence the cathodic reaction. On the other hand, the $J_{const.}$ value at −1.0 V increases with L929 cells (see figure 7*b*). Further investigation is necessary to understand the effect of cells and ECM on the H^+ reduction reaction.

The cathodic reaction in the body on implanted metallic biomaterials should be the reduction of dissolved oxygen according to the pH and Pourbaix diagram (Pourbaix 1974). Cathodic reaction always occurs as a counter reaction of anodic reaction, i.e. the dissolution of metal ions. The retardation of the cathodic reaction with adsorbed biomolecules and adhered cells influences the OCP because OCP is an equivalent point between cathodic and anodic reaction.

In this study, the OCP negatively shifts with cells, which is supported by the decrease in the cathodic current densities with cells. The difference in OCP between L929/316L and MEM+FBS/316L is small, probably because the surface is not fully covered with cells. A negative shift of OCP with L929 cells is also observed on Ti (Hiromoto *et al.* 2004). Therefore, the increase of the cell coverage on the surface is expected to enhance the decrease in OCP with cells. The OCP of 316L steel in the body is then supposed to be lower than that in a solution without cells. The corrosion rate and reactant in the corrosion reaction of metallic biomaterials depend on their OCP. Therefore, the OCP of metallic biomaterials *in vivo* needs to be investigated in order to simulate *in vivo* corrosion reaction outside of the body for the accurate elucidation of the corrosion behaviour.

4.2. Effects of biomolecules and L929 cells in a passive region of 316L steel

With biomolecules and cells, the OCP of 316L steel slightly decreases (see figure 3), and the passive current density increases (see figures 4*b* and 6). These results indicate that the protective ability of the passive film of 316L steel decreases with biomolecules and L929 cells because the interface environment becomes severe to the passive film.

The protective ability of the passive film depends on the following factors with biomolecules and L929 cells:

(i) The chemical environment, such as the oxygen concentration and pH near the surface.
(ii) The composition and thickness of surface oxide film, including inorganic precipitates.
(iii) The composition, amount, and conformation of the biomolecules and extracellular matrix adsorbed on the surface.

The decrease in the cathodic current density of around −0.5 V indicates that the oxygen concentration near the surface probably decreases with L929 cells. Hiromoto & Hanawa (2004) reported that the pH near L929 cells on 316L steel is low. These results indicate that the decrease in dissolved oxygen and low pH cause the formation of less protective passive film with cells than that without cells.

According to the surface analysis of 316L steel prepared in the same procedure as that in this study (Hanawa *et al.* 2002), there is not a significant difference in the relative concentration ratios of Fe to Cr, [Fe]/[Cr], on MEM+FBS/316L, L929/316L, and Hanks/316L. On the other hand, the precipitation of calcium phosphate on MEM+FBS/316L and L929/316L is 70% smaller than that on Hanks/316L (Hanawa *et al.* 2002). In addition, calcium phosphate precipitates not only on the passive film of 316L steel but also on the collagen fibre generated by L929 cells because calcium phosphate precipitates on collagen fibre generated by osteoblast cells (Kuboki *et al.* 1992). The decrease of calcium phosphate on the film would cause a decrease in the protective ability of the passive oxide film of 316L steel with biomolecules and cells.

The higher anodic J_{peak} values of MEM+FBS/316L and L929/316L than of Hanks/316L are caused by the acceleration of the charge transfer with biomolecules and L929 cells. Omanovic & Roscoe (1999) suggested that the acceleration of the charge transfer with adsorbed albumin causes a decrease in the protective ability of austenitic low-carbon stainless steel in a deaerated phosphate-buffered solution with immersion for 1.8 ks. The acceleration of the charge transfer with

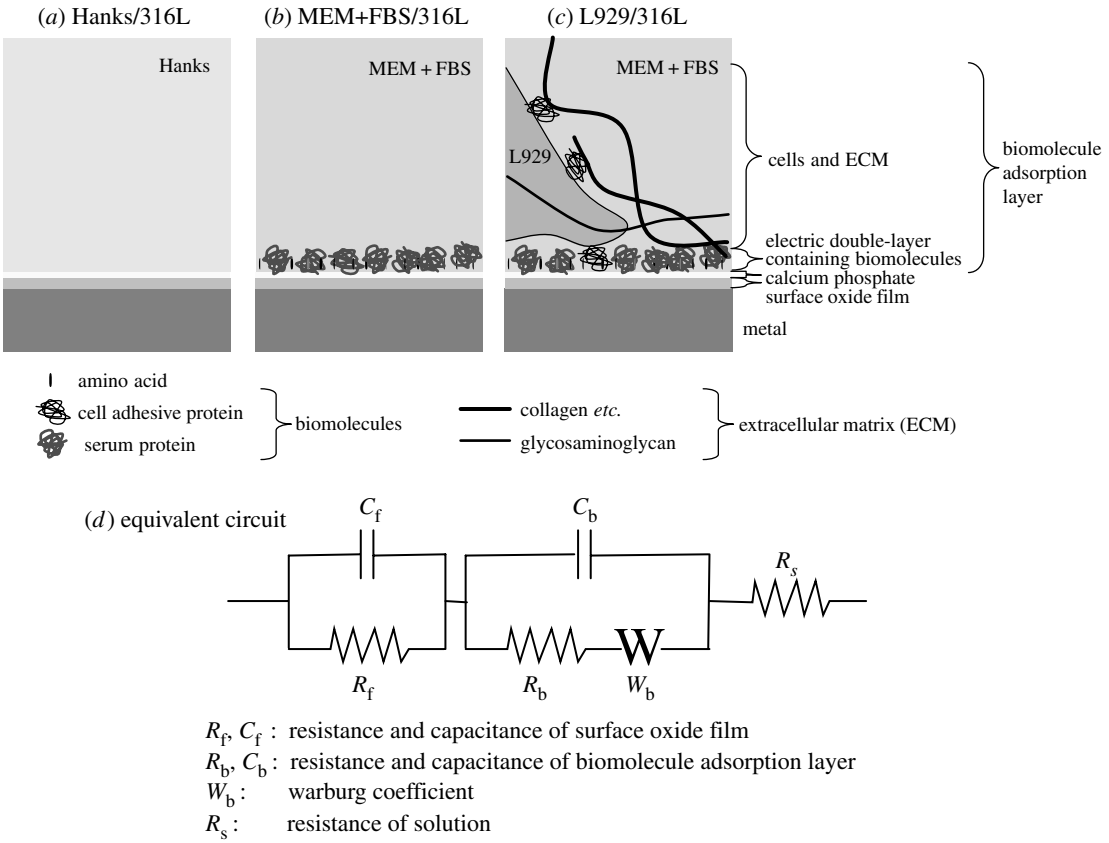

Figure 9. Schematic illustration of the assumed interface on 316L steel prepared in various environments and assumed equivalent electric circuit. (*a*) Hanks/316L, (*b*) MEM+FBS/316L, (*c*) L929/316L and (*d*) equivalent electric circuit.

adsorbed protein is also reported on Ti with fibrinogen (Jackson *et al.* 2000).

The anodic J_{peak} values increase with coated collagen in the comparison with the autoclaved specimen, indicating that the coated collagen accelerates the charge transfer as well as cells. Collagen is the main component of the extracellular matrix of L929 cells (Hayashi 1995; Lanza *et al.* 1997). These results suggest that the collagen coating can provide an environment for an anodic reaction similar to that under cell culture.

The pitting corrosion resistance of 316L steel decreases with biomolecules and L929 cells, as shown in the decrease in E_{pit} (see figure 5). The decrease in diffusivity at the interface with biomolecules and cells indicates that dissolved metal ions are accumulated at the interface, leading to an accumulation of chloride ion. On the other hand, the distribution of cells on the surface is not uniform (see figure 2). This suggests that the local corrosion is accelerated by the inhomogeneity of the surface due to the cells.

4.3. Effects of L929 cells in the impedance behaviour of 316L steel

The interface structures on 316L steel in various environments are assumed as shown in figure 9 according to the surface analysis data of 316L steel prepared in the same procedure as that in this study (Hanawa *et al.* 2002). On Hanks/316L, the surface of 316L steel is covered with oxide film, and calcium phosphate is precipitated. The concentrations of

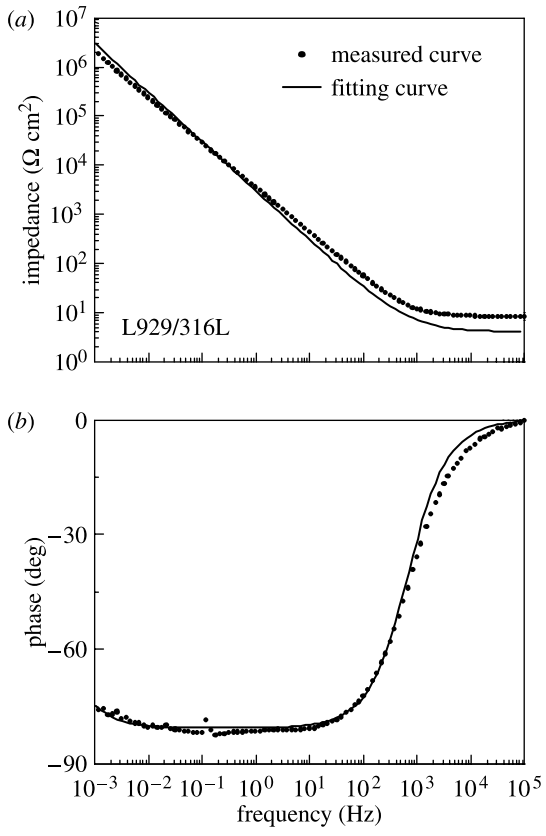

Figure 10. Z and phase shift curves measured and fitted to the equivalent electric circuit in figure 9*d* in the case of L929/316L.

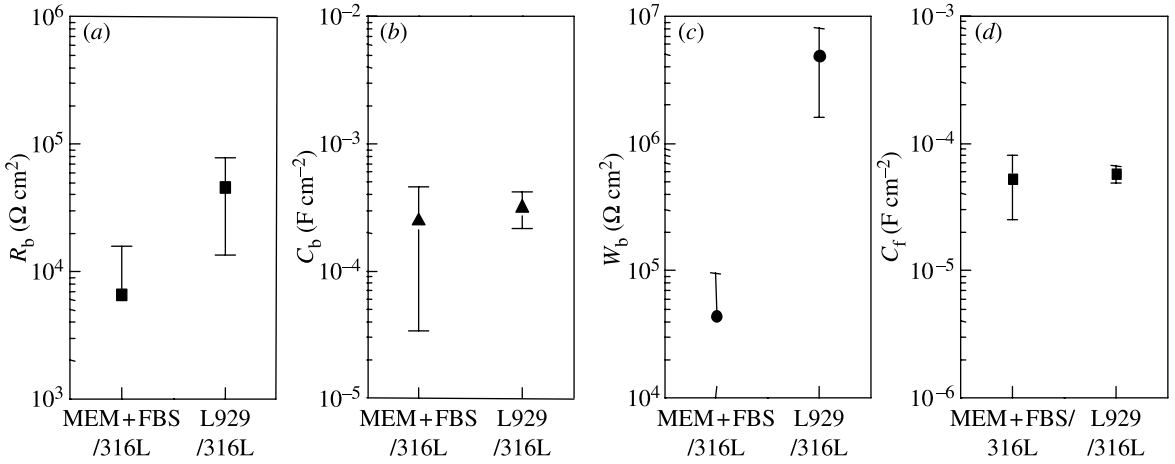

Figure 11. Approximated parameters on the equivalent electric circuit in figure 9*d*. (*a*) Resistance (R_b), (*b*) capacitance (C_b) and (*c*) Warburg coefficient (W_b) of the biomolecule adsorption layer and (*d*) capacitance of surface oxide film (C_f).

calcium and phosphate ions in the surface oxide film on Hanks/316L are 1.9 and 3.1 at.%, respectively (Hanawa *et al.* 2002), which would not be sufficient to uniformly cover the surface oxide film. On MEM+FBS/316L, in addition to calcium phosphate, amino acids and serum proteins are adsorbed on the surface. On L929/316L, L929 cells adhere on the surface with cell adhesive proteins, and the cells are surrounded with ECM generated by the cells. Calcium phosphate probably precipitates on the collagen fibre generated by L929 cells as well as on the surface oxide film because calcium phosphate precipitates on the collagen fibre generated by osteoblast cells (Kuboki *et al.* 1992).

When L929 cells fully and tightly cover the surface as a layer, the layer should exhibit a capacitance because both the cell membrane and intracellular fluid exhibit a capacitance (Ikeda 2000). However, L929 cells do not fully cover the surface in this study, indicating that the capacitance of L929 cells is included in that of the electric double-layer. The proteins are lying partly within the electric double-layer, and an electric double-layer is formed around the protein molecules (Ivarsson & Lundstrom 1986), indicating that the capacitance of biomolecules is included in that of electric double-layer. Therefore, the electric double-layer containing biomolecules and cells is described as a biomolecule adsorption layer (see figure 9). The biomolecule adsorption layer probably acts as a diffusion barrier according to the decrease in the cathodic current density with biomolecules and cells. In addition, the gel-like basement of ECM governs the diffusion of molecules (Alberts *et al.* 1990). The diffusion factor (Warburg coefficient) is then included in the equivalent circuit (see figure 9*d*).

The impedance data on Hanks/316L are not approximated to the assumed equivalent circuit in figure 9*d*. Hodgson *et al.* (2002) reported that the precipitated calcium phosphate shows a capacitive behaviour independently of the oxide film of Ti and Ti alloy immersed in a calcium phosphate saline solution. Although the precipitated amount of calcium phosphate on 316L steel is smaller than that on Ti (Hanawa *et al.* 2002; Hiromoto *et al.* 2004), the apparent two time constants on the impedance spectra indicate that the precipitated calcium phosphate exhibit an extra capacitance on Hanks/316L. On the other hand, Hanks/316L does not have a biomolecule adsorption layer. The adsorbed biomolecules are supposed to act as a diffusion barrier as reported on Ti (Hiromoto *et al.* 2002*a*,*b*). The L929 cells on 316L steel form a similar biomolecule adsorption layer to that on Ti because there is not a significant difference in the morphology of L929 cells on 316L steel and Ti. These indicate that the presence of a capacitance of calcium phosphate and the absence of a biomolecule adsorption layer is responsible for the discordance between the fitted and the measured curves. Another equivalent circuit with two capacitances and without a Warburg coefficient was then assumed for Hanks/316L because the impedance spectra indicate the existence of two time constants, however, the fitted curve did not show coincide to the measured curve. The other equivalent circuit should be assumed for Hanks/316L.

The approximated R_b increases with L929 cells. Huang (2004) reported that the polarization resistance obtained from the curve fitting of the impedance data to a certain equivalent circuit increases with the growth of osteoblast-like cell on Ti and Ti alloy. This result supports the increase in R_b with cells in this study. The approximated C_b and C_f values do not change with cells. Aoyagi *et al.* (2004) reported that the variety of proteins on the surface changes with L929 cells. However, the change in the variety of biomolecules in the layer does not directly influence the C_b value. Hanawa *et al.* (2002) reported that the composition of the surface oxide film of 316L steel does not significantly change with L929 cells. This result supports that the C_f value does not change with cells. On the other hand, the approximated W_b value apparently increases with L929 cells, indicating that the diffusivity at the interface decreases with cells.

The magnitude of the parameters in the equivalent circuit does not change with cells, except R_b and W_b. This result indicates that the culturing L929 cells do not drastically change the capacitive property of the oxide film of 316L steel. On the other hand, the protective ability of the passive oxide film and pitting corrosion resistance decrease with L929 cells.

According to the impedance behaviour, the culturing L929 cells influence the diffusivity at the interface. The decrease in diffusivity at the interface with L929 cells probably cause the deficient of dissolved oxygen as the cells consume oxygen and also the accumulation of chloride ion as the corrosion proceeds. These changes in the chemical environment at the interface with cell would lead to a decrease in the protective ability of the oxide film of 316L steel. However, further investigation is necessary to understand the effect of cells on the corrosion behaviour of 316L steel.

5. CONCLUSION

The effect of culturing murine fibroblast L929 cells on the corrosion behaviour of 316L stainless steel was investigated using polarization and impedance tests. The effect of type I collagen coating was also investigated using a potential step test. The results are summarized as follows:

(i) The protective ability of the passive oxide film and the pitting corrosion resistance of 316L steel decrease with L929 cells.
(ii) The cathodic current density for the reduction of dissolved oxygen decreases with L929 cells.
(iii) The culturing L929 cells and collagen coating on the surface cause an increase in the peak current density induced by the anodic potential step.
(iv) The diffusion parameter in the equivalent circuit increases with L929 cells.

Consequently, the corrosion resistance of 316L steel and the diffusivity at the interface decrease with L929 cells. The collagen coating possibly provides an environment for an anodic reaction similar to that with culturing cells.

We would like to thank Dr A. Yamamoto for her valuable advice concerning cells and cell culture and Ms F. Mizuno for her sincere assistant with the experiments.

REFERENCES

Alberts, B., Johnson, A., Lewis, J., Raff, M., Roberts, K. & Walter, P. 2002 The cell cycle and programmed cell death. In *Molecular biology of the cell*, 4th edn., p. 1015. New York: Garland Science/Taylor & Francis Group.

Alberts, B., Bray, D., Lewis, J., Raff, M., Roberts, K. & Watson, J. D. 1990 *Molecular biology of the cell*. Tokyo: Kyoiku-sha.

Aoyagi, S., Hiromoto, S., Hanawa, T. & Kudo, M. 2004 TOF–SIMS investigation of metallic material surface after culturing cells. *Appl. Surf. Sci.* **231-232**, 470–474. (doi:10.1016/j.apsusc.2004.03.181)

Dickinson, W. H., Lewandowski, Z. & Geer, R. D. 1996 Evidence for surface changes during ennoblement of type 316L stainless steel: dissolved oxidant and capacitance measurements. *Corros. Sci.* **52**, 910–920.

Esposito, M., Lausmaa, J., Hirsch, J. M. & Thomsen, P. 1999 Surface analysis of failed oral titanium implants. *J. Biomed. Mater. Res. Appl. Biomater.* **48**, 559–568. (doi:10.1002/(SICI)1097-4636(1999)48:4<559::AID-JBM23>3.0.CO;2-M)

Gilbert, J. L., Zarka, L., Chang, E. & Thomas, C. H. 1998 The reduction half cell in biomaterials corrosion: oxygen diffusion profiles near and cell response to polarized titanium surfaces. *J. Biomed. Mater. Res.* **42**, 321–330. (doi:10.1002/(SICI)1097-4636(199811)42:2<321::AID-JBM18>3.0.CO;2-L)

Hanawa, T., Hiromoto, S. & Asami, K. 2001 Characterization of the surface oxide film of a Co–Cr–Mo alloy after being located in quasi-biological environments using XPS. *Appl. Surf. Sci.* **183**, 68–75. (doi:10.1016/S0169-4332(01)00551-7)

Hanawa, T., Hiromoto, S., Yamamoto, A., Kuroda, D. & Asami, K. 2002 XPS characterization of the surface oxide film of 316L stainless steel samples that were located in quasi-biological environments. *Mater. Trans.* **43**, 3088–3092. (doi:10.2320/matertrans.43.3088)

Hayashi, M. 1995 *Cell-adhesive molecules (Saibo-Secchaku-Bunshi-no-Sekai)*, pp. 11–21. Tokyo: Yodo-sha.

Hiromoto, S. & Hanawa, T. 2004 pH near cells on stainless steel and titanium. *Electrochem. Solid-State Lett.* **7**, B9–B11. (doi:10.1149/1.1645353)

Hiromoto, S., Noda, K. & Hanawa, T. 2002*a* Development of electrolytic cell with cell-culture for metallic biomaterials. *Corros. Sci.* **44**, 955–965. (doi:10.1016/S0010-938X(01)00110-X)

Hiromoto, S., Noda, K. & Hanawa, T. 2002*b* Electrochemical properties of an interface between titanium and fibroblasts L929. *Electrochem. Acta* **48**, 387–396. (doi:10.1016/S0013-4686(02)00684-9)

Hiromoto, S., Hanawa, T. & Asami, K. 2004 Composition of surface oxide film of titanium with culturing murine fibroblasts L929. *Biomaterials* **25**, 979–986. (doi:10.1016/S0142-9612(03)00620-3)

Hodgson, A. W. E., Mueller, Y., Forster, D. & Virtanen, S. 2002 Electrochemical characterization of passive films on Ti alloys under simulated biological conditions. *Electrochim. Acta* **47**, 1913–1923. (doi:10.1016/S0013-4686(02)00029-4)

Huang, H.-H. 2004 *In situ* surface electrochemical characterizations of Ti and Ti–6Al–4V alloy cultured with osteoblast-like cells. *Biochem. Biophys. Res. Commun.* **314**, 787–792. (doi:10.1016/j.bbrc.2003.12.173)

Ikeda, K. 2000 *Seitai-bussei* (vital properties). In *Vital properties/medical mechanical engineering (Seutai-bussei/Iyou-kikai-kogaku)* (ed. K. Ikeda & H. Shimazu), pp. 18–25. Tokyo: Shujun-sha Co., Ltd.

Ivarsson, B. & Lundstrom, I. 1986 Physical characterization of protein adsorption on metal and metaloxide surfaces. *Crit. Rev. Biocompat.* **2**, 1–96.

Jackson, D. R., Omanovic, S. & Roscoe, S. G. 2000 Electrochemical studies of the adsorption behavior of serum proteins on titanium. *Langmuir* **16**, 5449–5457. (doi:10.1021/la991497x)

Kuboki, Y., Kudo, A., Mizuno, M. & Kawamura, M. 1992 Time-dependent changes of collagen cross-links and their precursors in the culture of osteogenic cells. *Calcif. Tissue Int.* **50**, 473–480. (doi:10.1007/BF00296780)

Lacour, F., Ficquelmont-Loïzos, M. M. & Caprani, A. 1991 Effect of the ionic strength of the supporting electrolyte on the kinetics of albumin adsorption at a glassy carbon rotating disk electrode. *Electrochim. Acta* **36**, 1811–1816. (doi:10.1016/0013-4686(91)85049-D)

Lanza, R. P., Langer, R. & Vacanti, J. 1997 *Principles of tissue engineering*, 2nd edn., pp. 57–71. California, USA: Academic Press.

Matsumoto, H. 1978 Interface phenomena on materials with good biocompatibility. *Chem. Rev.* **21**, 35–54.

Messer, R., Kimbrough, D., Austin, G. & Venugopalan, R. 2001 *In vitro* test system combining cell culture and corrosion techniques. In *Proc. Society for Biomaterials 27th Annual Meeting Transactions*, p. 221. Saint Paul.

Mustafa, K., Pan, J., Wroblewski, J., Leygraf, C. & Arvidson, K. 2002 Electrochemical impedance spectroscopy and X-ray photoelectron spectroscopy analysis of titanium surfaces cultured with osteoblast-like cells derived from human mandibular bone. *J. Biomed. Mater. Res.* **59**, 655–664. (doi:10.1002/jbm.1275)

Omanovic, S. & Roscoe, S. G. 1999 Electrochemical studies of the adsorption behavior of bovine serum albumin on stainless steel. *Langmuir* **15**, 8315–8321. (doi:10.1021/la990474f)

Pourbaix, M. 1974 *Atlas of electrochemical equilibria in aqueous solutions*, 2nd edn., pp. 97–105. TX, USA: NACE.

Stoner, G. & Srinivasan, S. 1970 Adsorption of blood proteins on metals using capacitance techniques. *J. Phys. Chem.* **74**, 1088–1094. (doi:10.1021/j100700a021)

Sundgren, J. L., Bodö, P. & Lundström, I. 1986 Auger electron spectroscopic studies of the interface between human tissue and implants of titanium and stainless steel. *J. Colloid Interface Sci.* **110**, 9–20. (doi:10.1016/0021-9797(86)90348-6)

Takemoto, S., Hiromoto, S., Mizuno, F., Hanawa, T., Ohnishi, I. & Nakamura, K. 2002 Surface analysis of metallic implant materials retrieved from patients. In *Proc. 24th Annual Meeting of the Japanese Society for Biomaterials*, p. 124, Tokyo, Japan.

Tamamushi, R. 2000 *Electrochemistry (Denki-kagaku)*, 2nd edn., pp. 193–292. Tokyo: Tokyo Kagaku Dojin.

Vinnichenko, M., Chevolleau, T. H., Pham, M. T., Poperenko, L. & Maitz, M. F. 2002 Spectroellipsometric AFM and XPS probing of stainless steel surfaces subjected to biological influences. *Appl. Surf. Sci.* **201**, 41–50. (doi:10.1016/S0169-4332(02)00290-8)

Wahlgren, M. & Arnebrant, T. 1991 Protein adsorption to solid-surfaces. *Trends Biotechnol.* **9**, 201–208. (doi:10.1016/0167-7799(91)90064-O)